# Supplementary material

## ERA5-Land analysis

Reanalysis data, including the variables 2m temperature, soil moisture layers 1-3, latent heat flux, LAI for high and low vegetation and downward solar radiation, from ERA5-Land from 1950 – 2020 were used to validate the CMIP6-based results[1,2]. All data has been aggregated to the monthly time scale and 2˚x2˚ spatial resolution. Maximum daily temperature was computed as the maximum average daily temperature per month. The root-zone soil moisture encompasses the soil moisture in top meter of the soil and is computed as a weighted average of soil moisture layers 1 (0 – 7cm), 2 (7 – 28cm) and 3 (28 – 100cm). The same methodology as has been applied to the CMIP6 data to compute temperature excess and ELI has been applied to the reanalysis data. Vegetated conditions were assumed when the LAI of either high or low vegetation > 0.5.

## Supplementary Figures

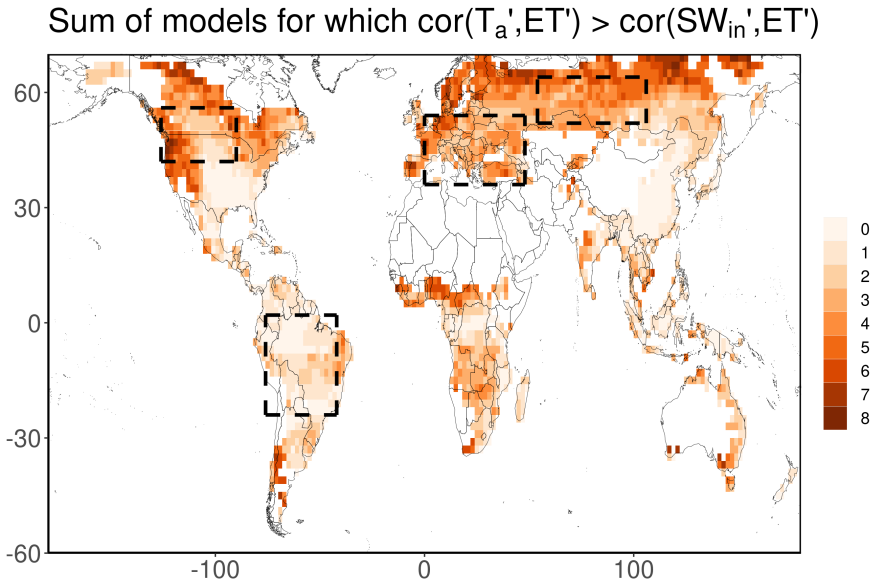


**Supplementary Figure 1: Spatial distribution of the sum of models that are temperature-controlled.** Colors show the sum of models for which cor($T_a$',ET') > cor($SW_{in}$',ET') over 1980 – 2100.

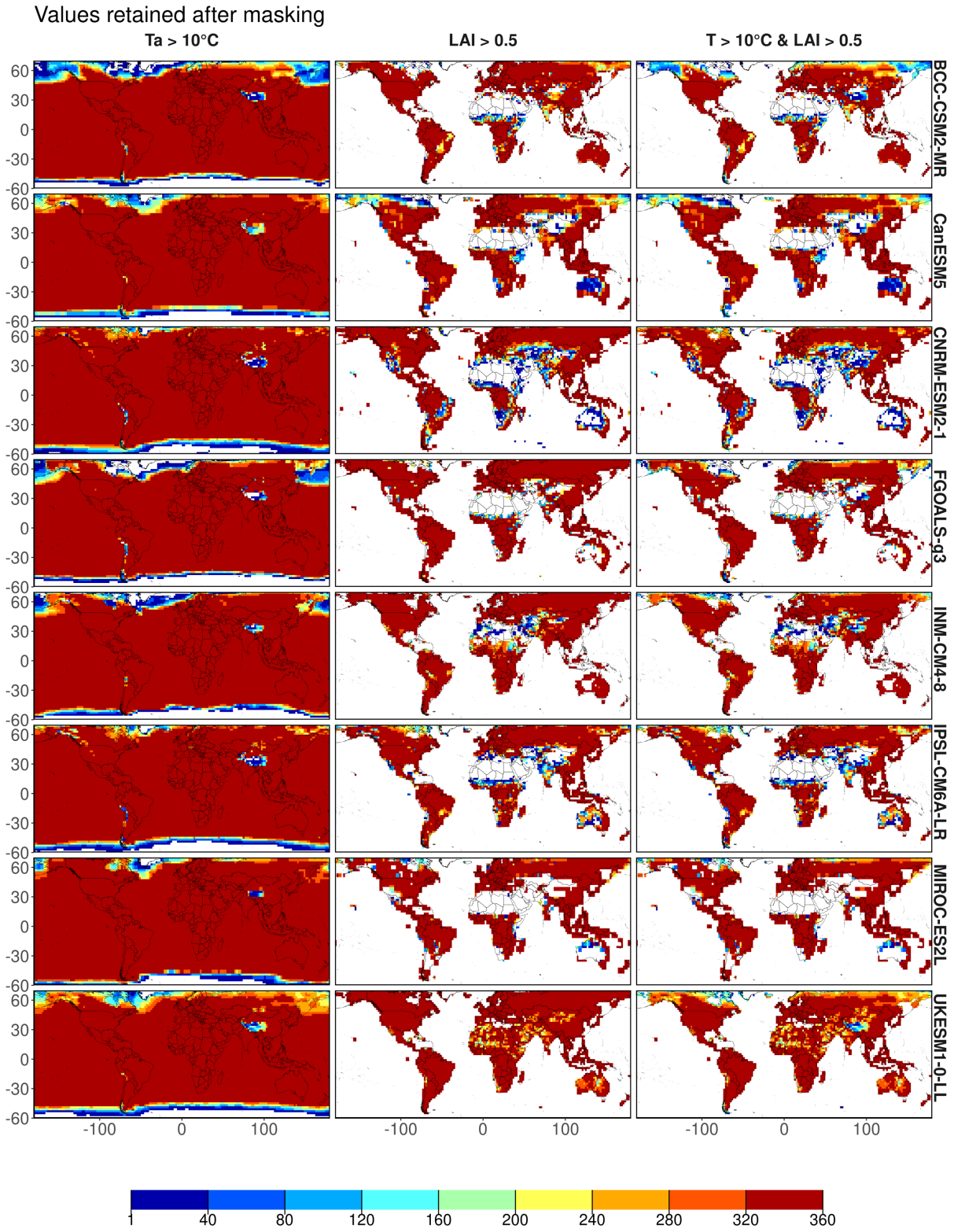


**Supplementary Figure 2: Data points retained after masking.** Columns denote the applied filtering procedures (from left to right: Ta < 10˚C, LAI < 0.5 and Ta < 10˚C & LAI < 0.5). Rows reflect the different individual models. The colors show the amount of values retained after filtering, where the maximum amount of values possible equals 3 hottest months per year over 120 years (360 data points). No data is available in the white regions.

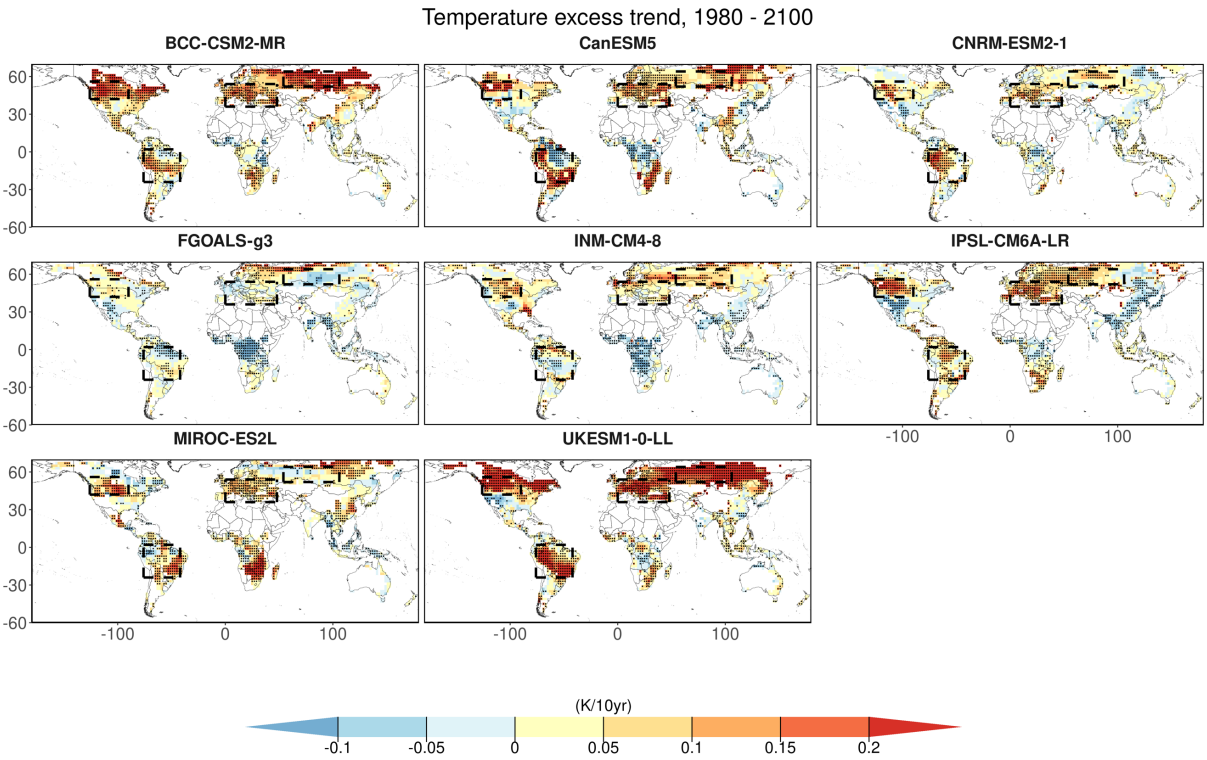


**Supplementary Figure 3: Trends of temperature excess for individual CMIP6 models.** The model-specific trends across decadal temperature excess time series (dots indicate significance: $p < 0.05$ based on Kendall's tau statistic).

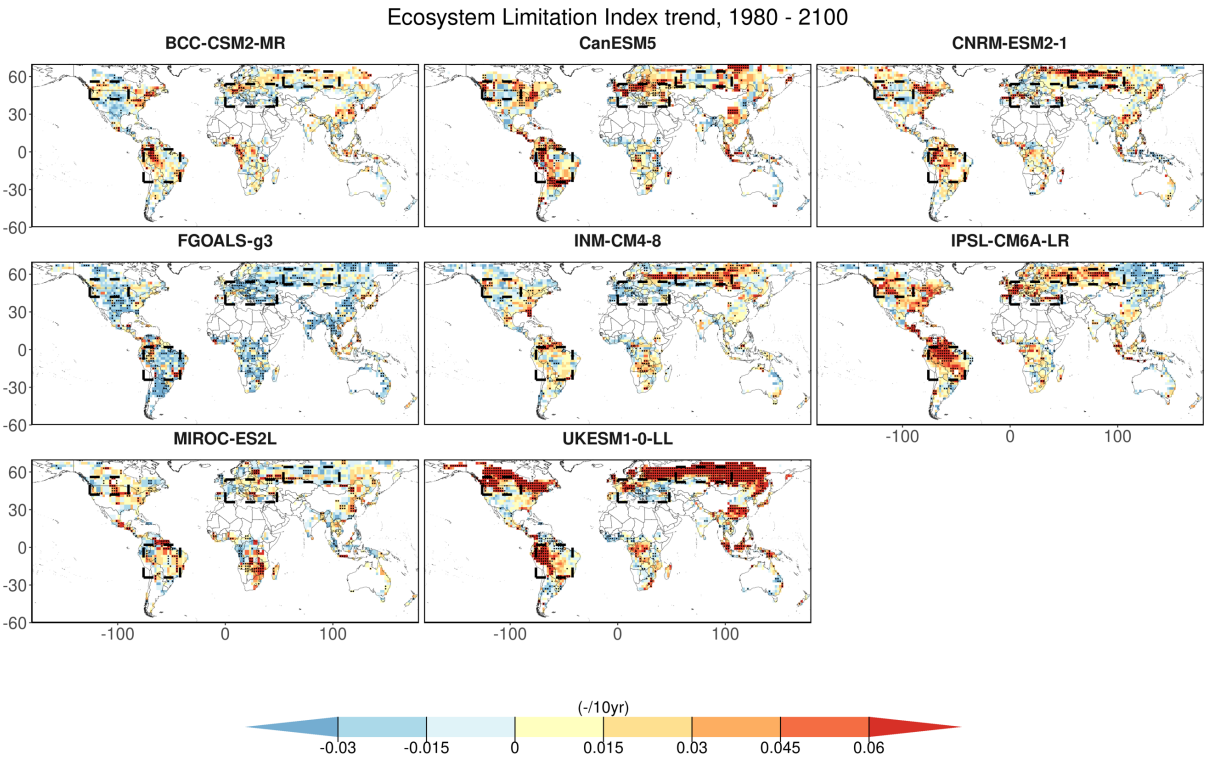


32

33 **Supplementary Figure 4: Trends in ecosystem water limitation for individual CMIP6**

34 **models.** The models-specific trends across decadal ELI time series (dots indicate significance:

35 $p < 0.05$ based on Kendall's tau statistic).

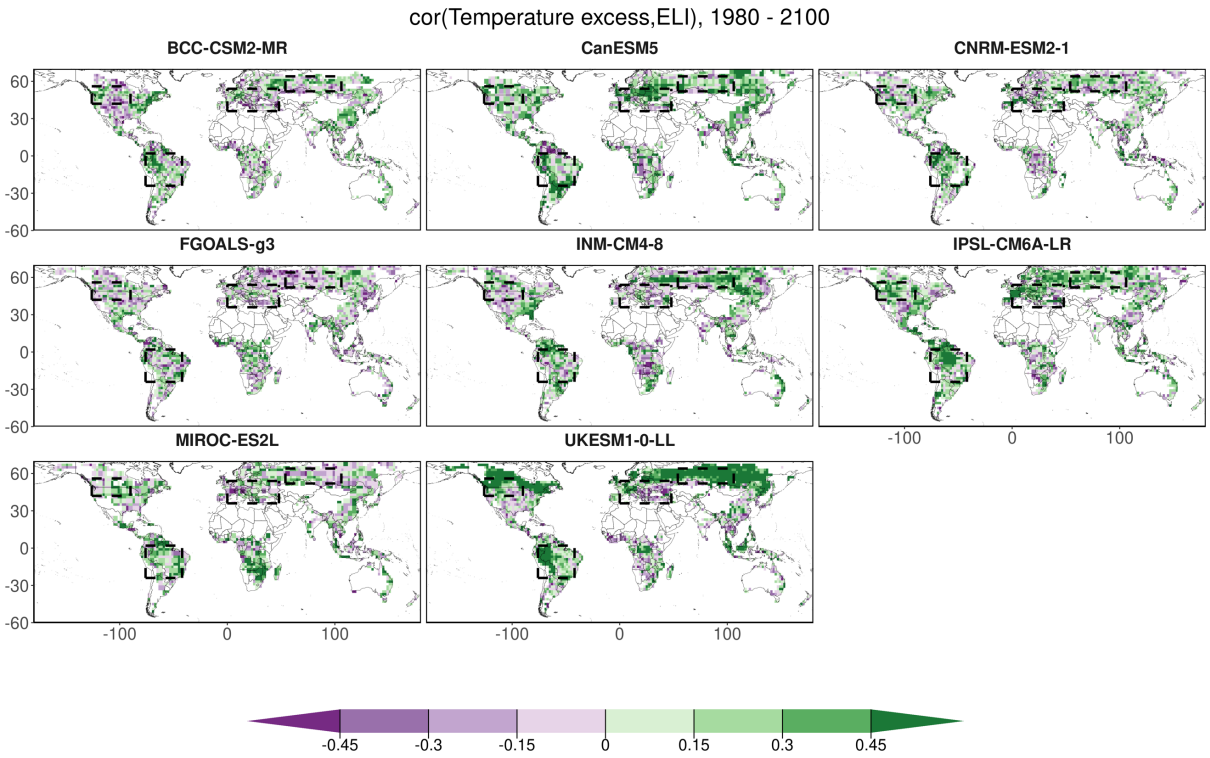


**Supplementary Figure 5: Kendall's rank correlation coefficient between ecosystem water limitation and temperature excess per individual CMIP6 model.**

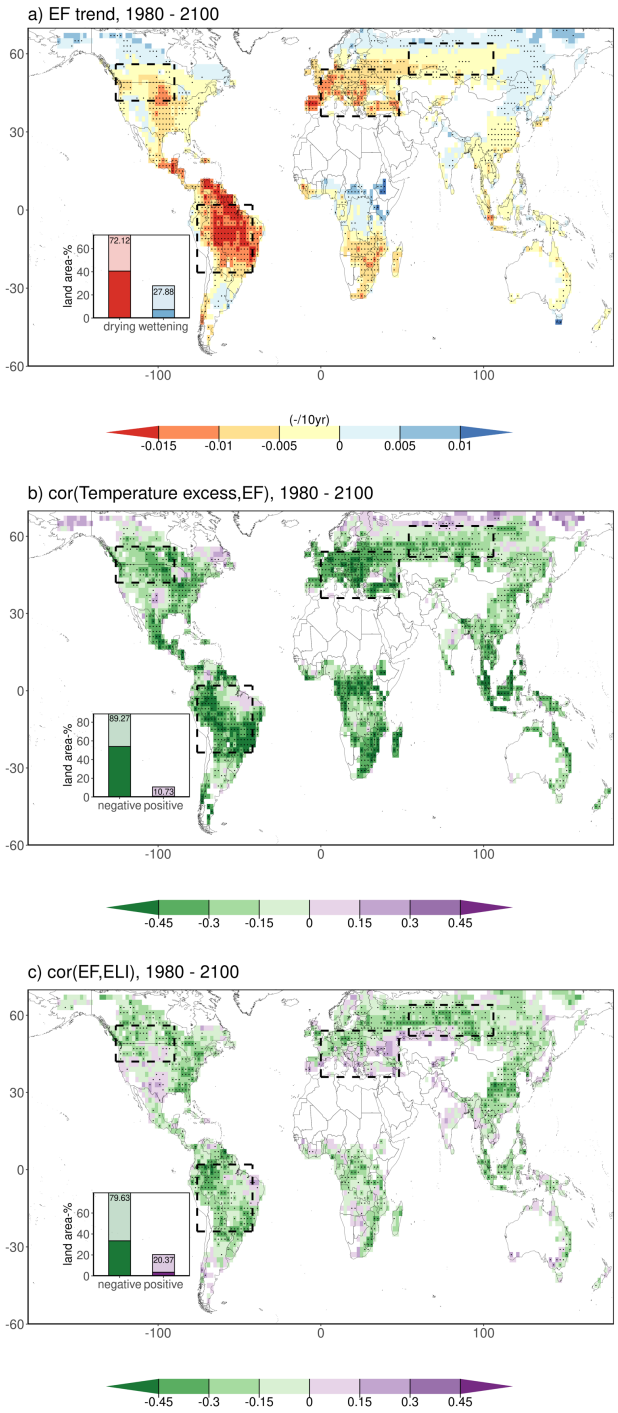


**Supplementary Figure 6: Global multi-model mean distribution and trends of Evaporative Fraction (EF).** Multi-model mean of trends based on decadal time series per respective CMIP6 model of a) EF and b) Ecosystem Limitation Index (ELI). c) Multi-model mean of Kendall's rank correlation coefficient between model-specific time series of ELI and temperature excess . The insets display the fraction of the warm land area that with positive or negative trends or correlations, respectively (at least 6 out of 8 models agreeing on the sign of

the trend or correlation are hued darker). Stippling indicates that at least 6 out of 8 CMIP6 models agree on the sign of the trend or correlation. All trends and correlations are calculated over the three hottest months-of-year, defined as the 3 months–of-year which have the highest average temperature over 1980 - 2100. The dashed boxes indicate regions of interest.

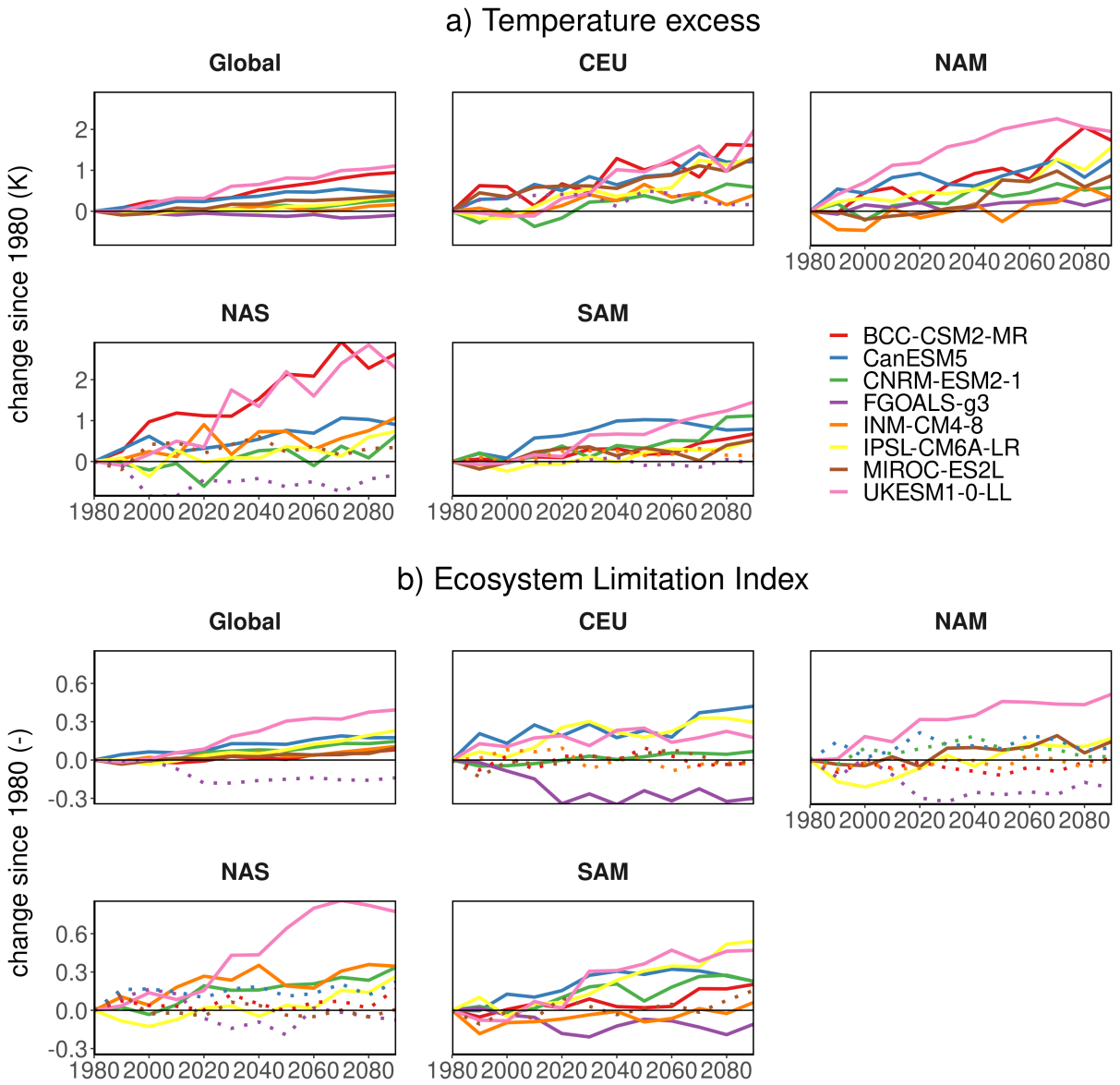


**Supplementary Figure 7: Model-specific changes in global and regional temperature excess in line with increasing ecosystem water limitation.** Temporal evolution of a) temperature excess and of b) Ecosystem Limitation Index (ELI) globally and for the regions of interest. Solid lines depict global and regional time series with significant trends ($p < 0.05$

based on Kendall's tau statistic). Global averages are calculated over land grid cells that have complete time series for all models and variables and are weighted according to the surface area per grid cell.

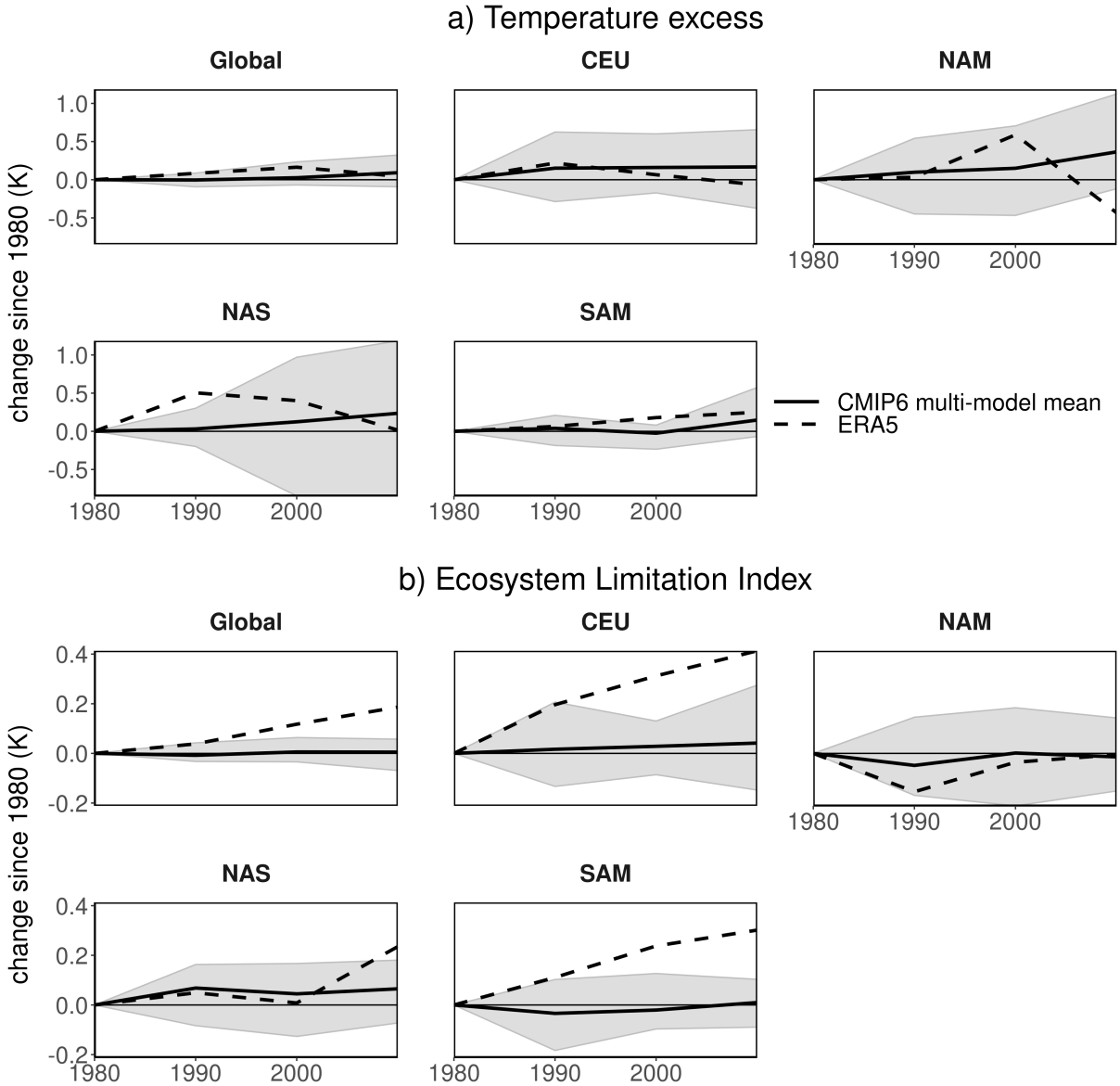


**Supplementary Figure 8: Changes in global and regional temperature excess in concert with increasing ecosystem water limitation from CMIP6 models and ERA5-Land.** Temporal evolution of a) temperature excess and of b) Ecosystem Limitation Index (ELI) globally and for the regions of interest. The black solid lines depict global and regional time from the CMIP6 models, while the black dashed line represent ERA5-Land. The grey ribbon

displays the envelope which encapsulates all the CMIP6 results. Global averages are calculated over land grid cells that have complete time series for all models and variables and are weighted according to the surface area per grid cell. The same mask is applied for CMIP6 models and ERA5-Land.

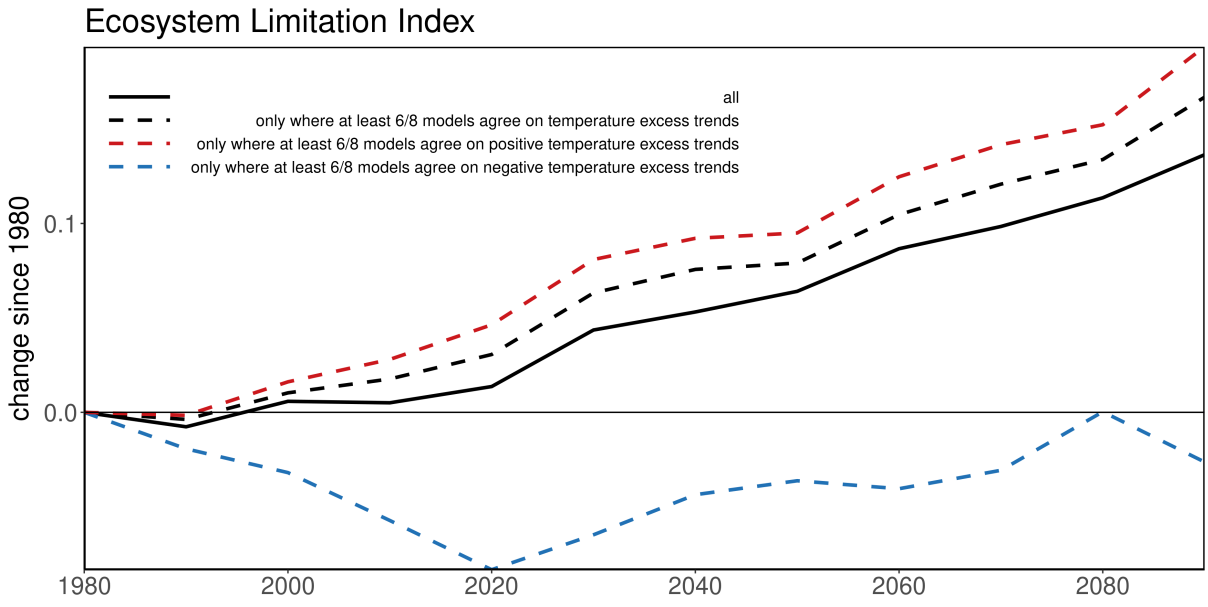


**Supplementary Figure 9: Contrasting trends of ecosystem water limitation from areas with different robustness of temperature excess.** All lines depict multi-model mean time series inferred from the model-specific time series. The solid black line is the same as in Figure 2b. The colored dashed lines only consider grid cells where at least 6 out of 8 CMIP6 models agree on temperature excess trends of either sign (black), positive (red) or negative (blue).

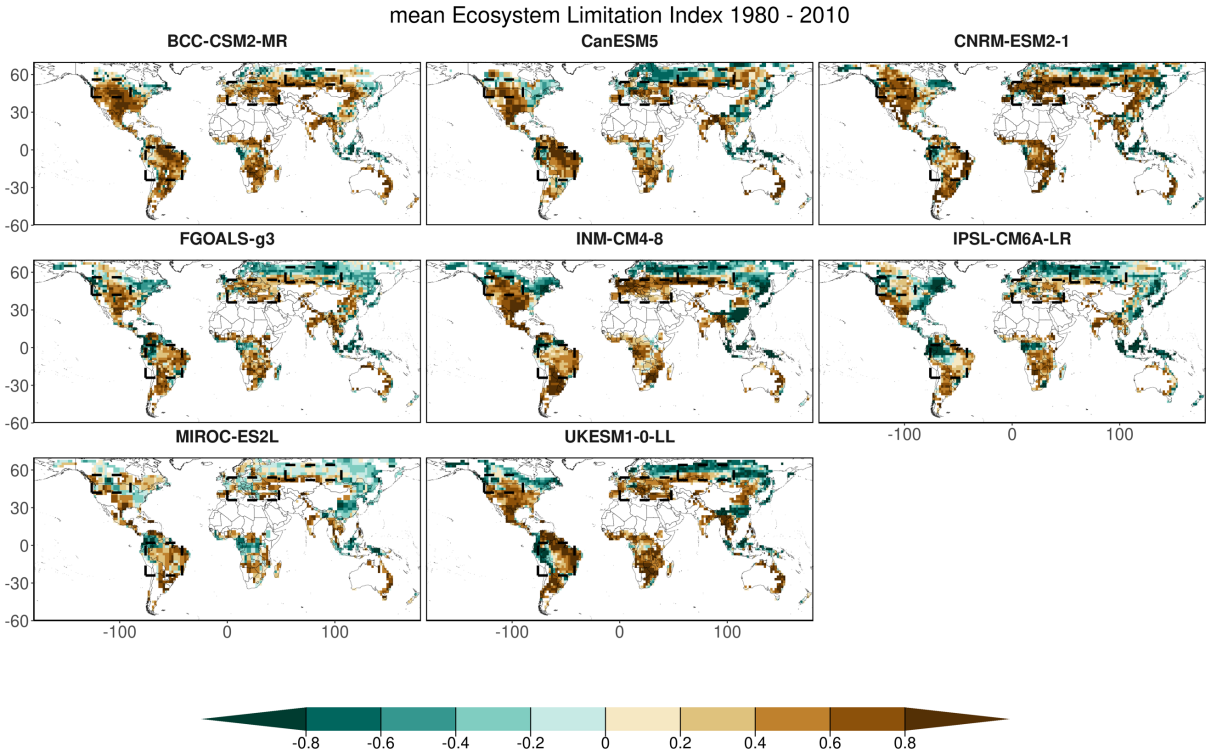


80

81 **Supplementary Figure 10: Model-specific initial ecosystem water limitation.** Model-

82 specific initial ELI averaged across 1980 - 2010.

83

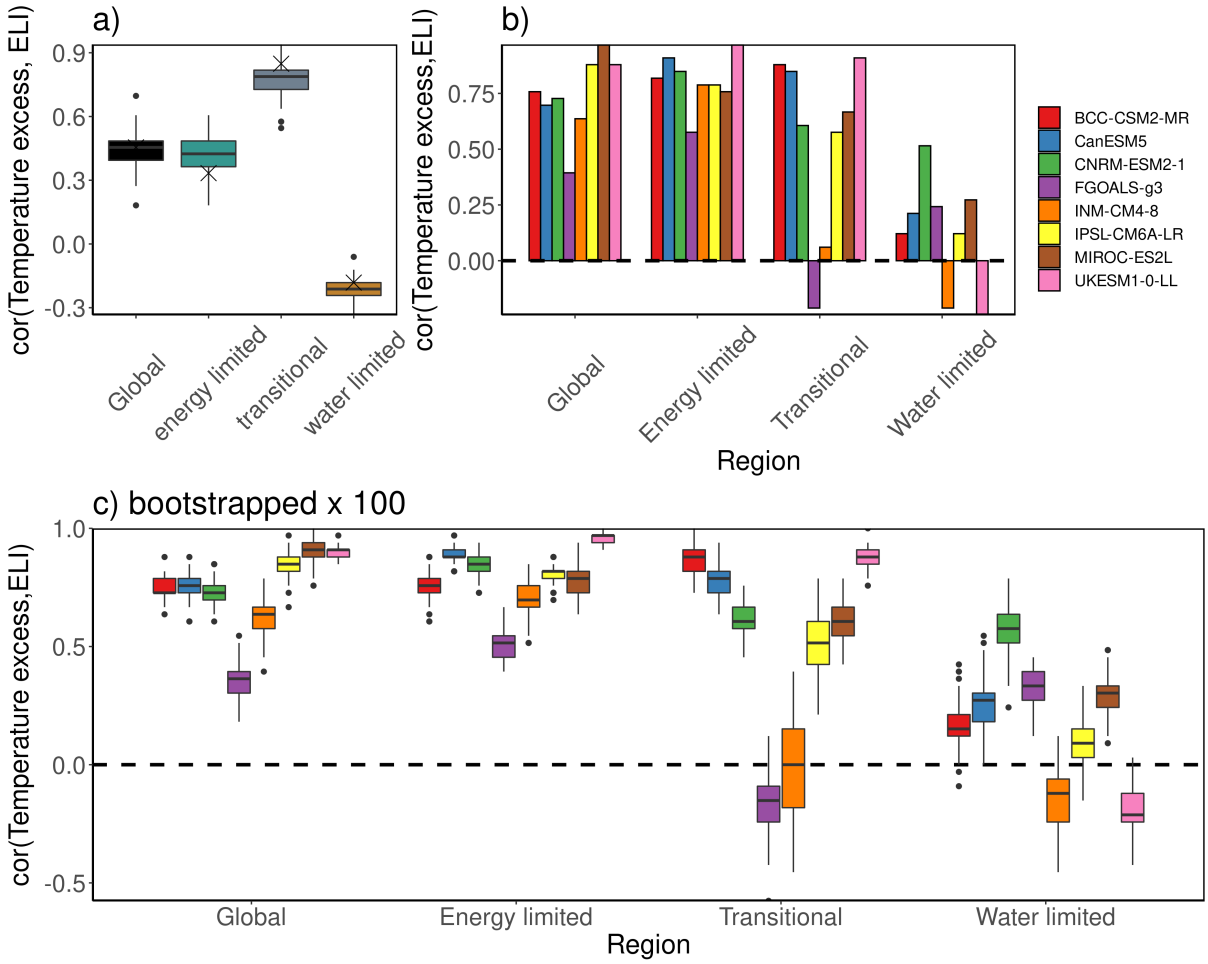


**Supplementary Figure 11**: **Model-specific global and regional correlations between temperature excess and ecosystem water limitation.** a) Correlations between decadal multi-model and regionally averaged time series of temperature excess and ELI, where crosses denote the correlation based on the original data and the box plots denote the uncertainty as obtained from bootstrapping (Methods). b) Barplots of correlations between decadal regionally averaged time series of temperature excess and ELI. c) The same as panel b), but with a hundred estimates obtained from bootstrapping. The regions are defined based on the mean ELI (1980 - 2010; Supplementary Figure 9): Energy limited (ELI < -0.2), transitional (-0.2 < ELI < 0.2) and water limited (ELI > 0.2).

## References

1. Muñoz Sabater, J. ERA5-Land monthly averaged data from 2001 to present. (2019) doi:10.24381/CDS.68D2BB30.

2. Muñoz-Sabater, J. *et al.* ERA5-Land: a state-of-the-art global reanalysis dataset for land applications. *Earth System Science Data* **13**, 4349–4383 (2021).